AL-ZAHRAA UNIVERSITY JOURNAL
Health and Medical Science

Al-Zahraa Journal for Health and Medical Sciences 2025; 3:1-21 **Vol. 3, No.3, 2025**
www.zjhms.alzahraa.edu.iq

Investigating the Structural, Electronic and Spectral Properties of Toxic Gases (CO, NO and H_2S) on the Al-doped Phosphorene Using Density Functional Theory

Mustafa Rahman Mohammed[1,a)], Rajaa K. Mohammad'[b)]

1) Physics Department, College of science, University of Kerbala, Karbala, Iraq.
*mustafa.rahman@s.uokerbala.edu.iq

Received: 24 June , Year (2025), Accepted: 08 August. 2025. Published: 30 Sept. 2025

ABSTRACT

To enhance the performance of phosphorene-based gas sensors made with aluminium-doped phosphorene. The study employed the Density Functional Theory (DFT) method for ground states to investigate the structural and electronic properties of toxic gases (CO, H_2S, and NO) adsorbed on Al-doped phosphorene surface compared with pristine phosphorene. Then, the Time-Dependent Density Functional Theory (TD-DFT) method for excited states was used to study the UV-vis spectrum. The results demonstrated that the nitrogen monoxide adsorbed on pure phosphorene surface as a NO/P showed the strongest adsorption, reaching to -2.3 eV, while nitrogen monoxide adsorbed on Al-doped phosphorene surface as a NO/Al-P showed the weakest adsorption, reaching to +1 eV. Furthermore, the energy gap of the Al-doped phosphorene (Al-P) reduced to 1.66 eV, while that of pure phosphorene (P) reached to1.73 eV. Based on the calculated energy gap values, the highest sensitivity for nitrogen monoxide adsorbed on the aluminium-doped phosphorene (NO/Al-P) surface reached to 40%, which is 10 times greater than the sensitivity of the sensor for pristine phosphorene (NO/P) at 4%. UV-Vis spectroscopic characteristics observed that the spectrum shifts towards the infrared region, extending from 3200 to 9400 nm. Our study proposes a simple and effective strategy for producing high-performance phosphorene-based gas sensors for nitrogen monoxide detection.

KEYWORDS: Phosphorene, Al-phosphorene, Nanosensor, DFT, TD-DFT.

AL ZAHRAA UNIVERSITY JOURNAL
Health and Medical Science

Al-Zahraa Journal for Health and Medical Sciences 2025; **3**:1-21 **Vol. 3, No.3, 2025**
www.zjhms.alzahraa.edu.iq

INTRODUCTION

Research on two-dimensional (2D) nanomaterials has seen rapid growth, motivated by their unique properties across several applications in biomedicine, supercapacitors, gas sensors, et cetera [1–4]. In 1914, under high-pressure and temperature experiments of 1.2 GPa and 200 °C, respectively. American physicist Percy Williams Bridgman successfully discovered phosphorus layers (phosphorene) that are linked together via van der Waals forces [5,6]. Whereas a substantial portion of its bulk semiconducting properties has been under investigation for a century [7], it is only recently that the few-layer phosphorene (P) structure has appeared in the scientific limelight [8]. Phosphorene has a distinct puckered structure, fully contented valence shell results in a direct energy gap, around 0.3–2 eV [9]. Furthermore, the tunable direct energy gap of phosphorene is ideal for optoelectronics covering the infrared to visible regions, giving the possibility of favorable photo detection capabilities extending from the visible to the infrared spectrum [10]. Carbon monoxide (CO) is a toxic gas emitted into the environment when carbonaceous materials are incompletely burned [11]. Hydrogen sulfide (H_2S) is a foul-smelling, toxic gas commonly found in the environment, released from geothermal vents and produced as a by-product in industries such as oil refining [12]. Nitrogen monoxide (NO) is a colorless highly reactive toxic gas. Industrially, it has several uses, for instance, as a product of the incomplete combustion of fossil fuels, for example, in motor vehicles (diesel and petrol fuels) and power stations [13]. Numerous studies have been undertaken to enhance the performance of pristine phosphorene as a sensor. This enhancement involves the substitution of certain atoms within the phosphorene structure with alternative atoms, aimed at improving its structural and electronic properties in order to investigate the feasibility of utilizing it as a gas sensor. For instance, Hosseini, S. in 2025 [14]. The study utilized density functional theory DFT method with LDA and GGA computations to examine the adhesion of CH_4, H_2S, and NH3 molecules to a single layer of phosphorene. The LDA approximation was used for structural optimization, while the GGA approximation was employed for an accurate description of intermolecular and van der Waals interactions. The study concluded that high sensitivity to gas

IRAQI Academic Scientific Journals

AL ZAHRAA UNIVERSITY JOURNAL
Health and Medical Science

Al-Zahraa Journal for Health and Medical Sciences 2025; 3:1-21 **Vol. 3, No.3, 2025**
www.zjhms.alzahraa.edu.iq

adsorption of phosphorene, makes it an excellent gas sensor and shows its potential for use in electronic devices. He, H. *et al*, [15]. A study conducted a systematic study on the sensing properties of the Au-P monolayer to several toxic gases (CO, H_2S, NO, NO_2, and SO_2) using density functional theory (DFT) and the non-equilibrium Green's function (NEGF) approach. The results demonstrate that the Au-P sensor enables ultra-sensitive removal of NO_x, which makes the Au-P monolayer nanostructure effective for applications in toxic gas sensing, especially NO_x detection. Ou *et al*, [16]. The study nominated monolayer phosphorene as a high-performance sensor material for volatile organic compounds (VOCs), such as ethanol, propionaldehyde, acetone, toluene, and hexane, employing a combination the DFT and NEGF environments. The results suggest that phosphorene is a compelling and feasible candidate for VOC sensing applications. In this article, the researcher presented the results of DFT calculations performed using the GaussView 6.0.16 and Gaussian 09W [17, 18] software at hybrid functional B3LYP and 6-31G basis set, which investigated the impact of the aluminum-doped monolayer phosphorene and its effectiveness in detecting the (H_2S, NO, and CO) as toxic gas molecules by studying the impact of the gas molecules on the structural, electronic, and spectral properties of pure and Al-doped phosphorene nanostructure.

COMPUTATIONAL METHODS

The DFT method was used to guesstimate the ground-state properties by utilizing a combination of GaussView 06 and Gaussian 09W software, which provides the required data about the HOMO-LUMO energy levels, energy gap, ionization energy, potential energy, adsorption energy, and sensitivity. On the other hand, the time-dependent density functional theory (TD-DFT) method was also used to estimate the excited-state properties by using a combination of GaussView 06 and Gaussian 09W software, which provides the required data about the Ultraviolet-Visible (UV-Vis) spectrum and helped identify the maximum wavelength of absorption (λ_{max}). All calculations are done using the hybrid functional B3LYP (Becke 3-parameter Lee–Yang–Parr) [18,19], which clarifies the exchange-correlation functional at the level of theory 6-31G basis set [20,21].

IRAQI Academic Scientific Journals

AL ZAHRAA UNIVERSITY JOURNAL
Health and Medical Science

Al-Zahraa Journal for Health and Medical Sciences 2025; 3:1-21 **Vol. 3, No.3, 2025**
www.zjhms.alzahraa.edu.iq

The DFT method is a computational simulation used in the science of nanomaterials, and it is commonly used for expecting and understanding the electronic nanostructures of various nanomaterials. By solving KS equations, this method employs exchange-correlation functional to account for electron-electron interactions, making it highly effective for investigating a broad spectrum of nanomaterials. So, the DFT method enabled researchers to evaluate the ground-state properties of many-electron system with balanced accuracy and computational efficiency. The scientists Kohn and Sham developed the practical rough calculation method of the ion state in a many-electron system named the Kohn-Sham equation [22]:

$$\left[-\frac{\hbar}{2m}\nabla^2 + V_{eff.}(r)\right]\phi_i(r) = \varepsilon_i\phi_i(r) \qquad \dots (1)$$

where ε_i: Energy eigenvalue of a many-electron (N-electrons) system.

$\phi_i(\mathbf{r})$: Wave function of a many-electron system $\phi_i(\mathbf{r_1}, \mathbf{r_2}, \mathbf{r_3}, \dots, \mathbf{r_N})$.

$V_{eff.}(\mathbf{r})$: Effective potential.

The equation of the effective potential of a many-electron system is given by:

$$\mathbf{V_{eff.}(r) = V_{ext.}(r) + V_H[n] + V_{xc}[n]} \qquad \dots (2)$$

Where $V_H[n]$: Hartree potential of a many-electron system.

$V_{xc}[n]$: Exchange-correlation potential of a many-electron system.

$V_{ext.}(\mathbf{r})$: External potential.

n(r): Electronic density.

The electronic density of an N-electron system n(r) was obtained from the Kohn-Sham orbitals as:

$$\boldsymbol{n(r) = \sum_{i=1}^{N} |\phi_i(r)|^2} \qquad \dots (3)$$

The sequence of steps involved in simulating the KS equation. The initial step is an option ***n(r)***, should it be utilized. The subsequent step concerns the effective potential $V_{eff.}(\boldsymbol{r})$ is predictable

IRAQI Academic Scientific Journals

AL ZAHRAA UNIVERSITY JOURNAL
Health and Medical Science

Al-Zahraa Journal for Health and Medical Sciences 2025; 3:1-21 **Vol. 3, No.3, 2025**
www.zjhms.alzahraa.edu.iq

using an approach as the local density approximation (LDA) and the generalized gradient approximation (GGA) for the exchange-correlation potential [23]. Furthermore, the wave function ϕ (**r**), which is used to evaluate the electronic density of a many-electron system n(**r**), it's also used to determine the attained $V_{eff.}(\mathbf{r})$ [24].

RESULTS AND DISCUSSION

The structural properties of pristine phosphorene were first explored, as illustrated in Figure 1, which shows the crystal structure of pure and Al-phosphorene. It can be seen that the monolayer phosphorene consists of two atomic planes, and the unit cell of phosphorene consists of four P atoms. The monolayer phosphorene has the bond length of the P–P bond in the horizontal direction (l_1) is 2.263 Å, and the length in the other direction (l_2) is 2.225 Å. Whereas the energy gap for pure phosphorene is 1.73 eV. It has also been modified on the monolayer phosphorene (**P)** by replacing a single aluminum Al atom with a phosphorus atom to get Al-phosphorene **Al-P** nanostructure with a band gap of 1.66 eV.

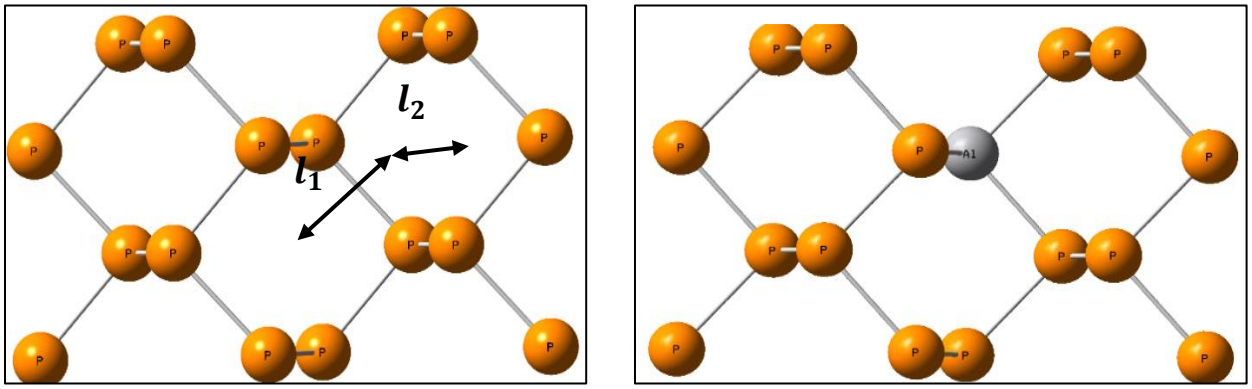

Figure 1. The structures of a pure and Al-doped phosphorene (P and Al-P) at B3LYP hybrid functional and 6-31G basis set. The orange balls include the phosphorus atoms, while the silver ball refers to the aluminum atom.

Figure 2 explains a simulation of monolayer phosphorene's pristine and doped structure (**P** and **Al-P),** respectively. It was also simulated for the **P** and **Al-P** nanostructures after adsorbing the gas molecules under study [34], as illustrated in the HOMO-LUMO level of states.

IRAQI Academic Scientific Journals

AL ZAHRAA UNIVERSITY JOURNAL
Health and Medical Science

Al-Zahraa Journal for Health and Medical Sciences 2025; 3:1-21 **Vol. 3, No.3, 2025**
www.zjhms.alzahraa.edu.iq

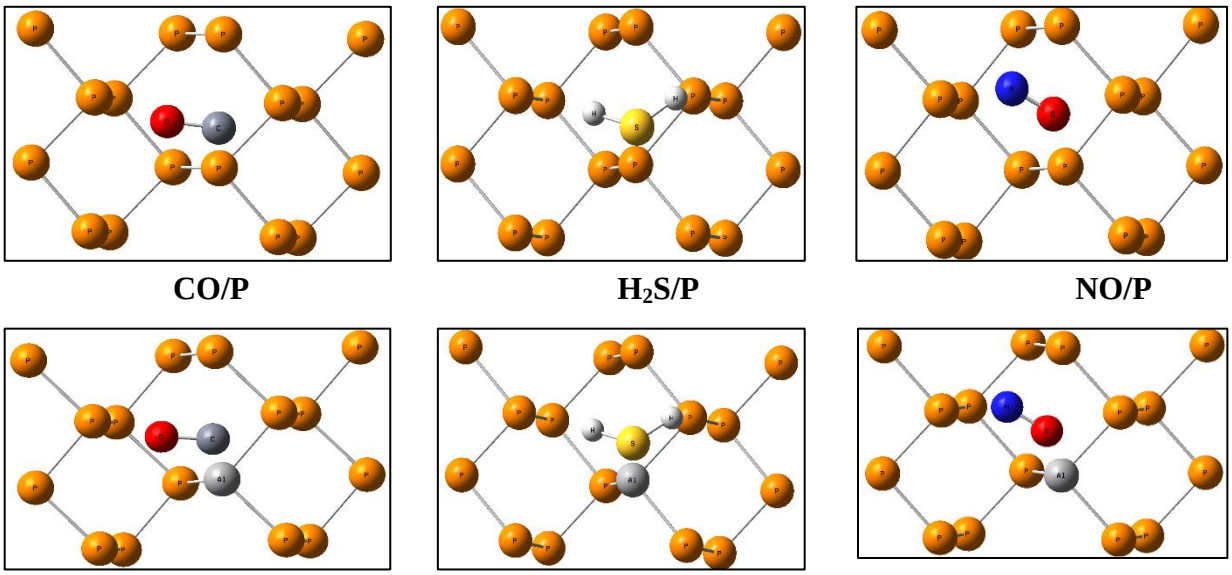

Figure 2. The geometrical nanostructures for the adsorbed CO, NO, and H_2S gas molecules on the pure and Al-phosphorene (P, Al–P) at B3LYP/6-31G computational environment, where the yellow, deep gray, red, blue, and white colors refer to sulfur, carbon, oxygen, nitrogen, and hydrogen atoms respectively.

The analysis of the crystal structure of **CO/Al-P** upon adsorption of carbon monoxide gas was optimized to be almost similar to the crystal structure before adsorption Al-P, which indicates that there is no substantial effect of CO gas on the crystal structure of the Al-phosphorene, which remains the most stable. Modifying the ground state energy for both **H_2S/Al-P,** and **NO/Al-P** involved approximating a H_2S, and NO gas molecule from the aluminum atom in a Al-phosphorene structure, different from a pure **H_2S/P,** and **NO/P** nanostructure, as will be shown later when interpreting HOMO-LUMO energy levels. The predominant characteristic observed across all instances except CO/Al-P was the absence of the original phosphorene monolayer preserved. Therefore, the molecular arrangement to be analyzed in the case of **NO/Al-P** was the most affected by those in the **H_2S/Al-P** case. In terms of geometric features, the aluminum atom created bonds with the neighboring P atoms, thus creating deformations among P-P bonds of the nanostructure [25], as will be shown later when interpreting HOMO-LUMO energy levels.

IRAQI Academic Scientific Journals

AL ZAHRAA UNIVERSITY JOURNAL
Health and Medical Science

Al-Zahraa Journal for Health and Medical Sciences 2025; 3:1-21 **Vol. 3, No.3, 2025**
www.zjhms.alzahraa.edu.iq

ADSORPTION ENERGY

The adsorption energy of a gas molecule under study on the surface of a pure and Al-doped phosphorene nanostructure is calculated to examine the stability of the adsorption systems using the following relationship [25,26]:

$$\mathbf{E_{ads} = E_{tot.} - (E_{gas} + E_{comp.})} \quad \ldots(4)$$

Where $E_{tot.}$ is the total energy of the adsorbed composite nanostructure after approximating a gas molecule, $E_{comp.}$ refers to the energy of either pure or Al-doped phosphorene (composite nanostructure), and E_{gas} denotes the energy of the toxic gases (CO, H_2S, and NO).

Based on this equation, a larger adsorption energy indicates a more stable structure, which is clearly shown in CO/P, NO/P, and H_2S/Al–P nanostructures respectevily. The Al-doped phosphorene Al–P demonstrated the highest adsorption for H_2S gas molecule around –2.11 eV, while the CO gas molecule provided the weakest physisorption (+1 eV) [27]. Likewise, a pure phosphorene demonstrated the highest adsorption for NO gas molecule around –2.3 eV, while the CO gas molecule provided the weakest physisorption (–0.19 eV). The adsorption energy is a common indicator of the strength of binding of the adsorbate to the substrate. If the adsorption is thermodynamically favorable, the energy of the whole adsorption system will be lower compared to the sum of the energy of the substrate and the adsorbate. Resulting in a negative adsorption energy value. Depending on the magnitude of the adsorption energy value, it is possible to determine the system physisorption or chemisorption process. It is worth noting that in simulating the adsorption system to calculate the adsorption energy, the substrate, and the adsorbate must use the same exchange-correlation function to improve the comparability of the calculation and to perform geometric relaxation [28]. There are usually three convergence criteria, i.e., energy, force, and atomic displacement. Every substrate provides the possibility to provide several various adsorption sites and usually requires an adsorption site test prior to testing, where the adsorbate is most likely to adhere to the lowest energy site [29], as shown in Figure 3.

IRAQI Academic Scientific Journals

AL ZAHRAA UNIVERSITY JOURNAL
Health and Medical Science

Al-Zahraa Journal for Health and Medical Sciences 2025; 3:1-21 Vol. 3, No.3, 2025
www.zjhms.alzahraa.edu.iq

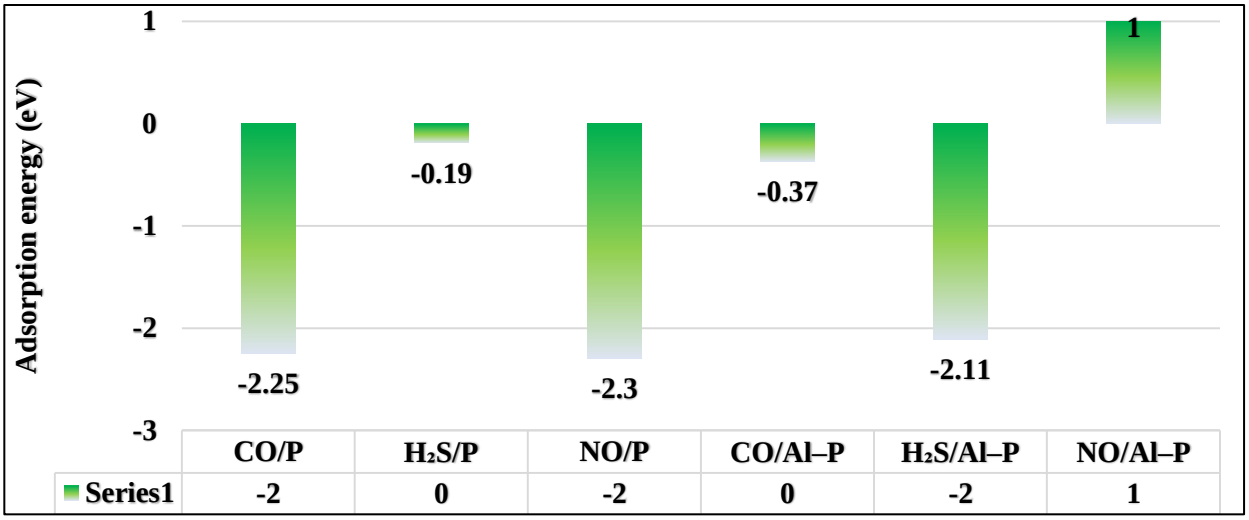

Figure 3. The adsorption energies of CO, NO, and H_2S molecules on pristine and aluminium-doped phosphorene (P and Al-P) structures at the hybrid functional B3LYP and 6-31G basis set.

Energy GAP

The energy bandgap of a semiconductor nanomaterial can be calculated as follows [30]:

$$E_g = E_{LUMO} - E_{HOMO} \quad \ldots (7)$$

Where E_{HOMO} and E_{LUMO} represents the highest occupied molecular orbital (HOMO) and the lowest unoccupied molecular orbital (LUMO) energy levels (eV), respectively [31]. So, E_g are parameters of importance for any electronic nanomaterial, be it a metal, semiconductor, or insulator. To a large range, these parameters are key components that define the electronic structure of all interfaces among bulk conventional to nanostructured materials, through control processes of charge exchanges inside the crystal structure for the nanostructured materials.

Figure 4 indicates the energy gap of the pure and Al-doped phosphorene nanostructures, as well as for their adsorption with gas molecules under study. The energy gap for the pure phosphorene structure is 1.73 eV, which was well compatible with the limit of measurements (0.3 – 2 eV) from bulk conventional to nanostructure of monolayer phosphorene [32]. On the other hand, the energy gap decreases after doping with an aluminium atom from 1.73 to 1.66 eV. The energy gap further decreases for $NO/Al-P$ nanostructure to 1 eV compared with the NO/P

IRAQI Academic Scientific Journals

AL ZAHRAA UNIVERSITY JOURNAL
Health and Medical Science

Al-Zahraa Journal for Health and Medical Sciences 2025; 3:1-21 **Vol. 3, No.3, 2025**
www.zjhms.alzahraa.edu.iq

structure,while it increases for the H_2S/Al–P nanostructure to 1.733 as compared with the pure H_2S/P structure, respectively [33].

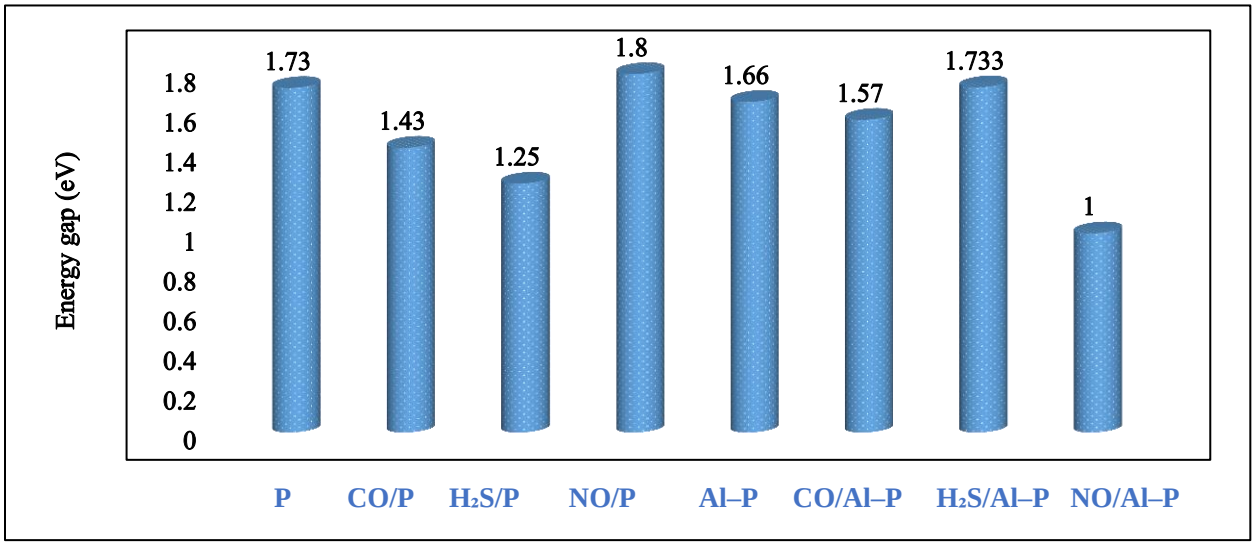

Figure 4. The energy bandgap of pristine and Al-doped phosphorene structures with and without CO, NO, and H_2S molecules at the hybrid functional B3LYP and 6-31G basis set.

The sensing capability of the Al–P sensor for the various gas molecules is assessed by quantifying its sensitivity, which can be expressed as follows [34]:

$$\mathbf{S}(\%) = \frac{|\mathbf{E} - \mathbf{E_0}|}{\mathbf{E_0}} \qquad \ldots(\mathbf{8})$$

Where E_0 refers to the energy bandgap of the nanosensor before the adsorption, while E denoted the energy bandgap of the nanosensor during the detection of the toxic gas molecules.

The results in Figure 5 indicate the sensitivity values for toxic gases when they are adsorbed on the surface of a pure and Al-doped phosphorene nanosheet. As is clear, the sensitivity of CO, H_2S, and NO gas molecules on the surface of the pristine phosphorene P nanosheet are computed to be 17%, 28%, and 4%, respectively. But, after being doped with an aluminium atom, the sensitivity of CO, H_2S, and NO gas molecules on the surface of Al − P structure are calculated to be 5%, 4%, and 40%, respectively. So, the sensitivity of the NO gas molecule on the surface of Al − P nanostructure is 10 times as large as compared to the adsorbed it on the surface of a pure

IRAQI Academic Scientific Journals

AL ZAHRAA UNIVERSITY JOURNAL
Health and Medical Science

Al-Zahraa Journal for Health and Medical Sciences 2025; 3:1-21 **Vol. 3, No.3, 2025**
www.zjhms.alzahraa.edu.iq

phosphorene. Whereas, the sensitivity of the H_2S gas molecule on the surface of $Al-P$ structure is 7 times smaller as compared to the adsorbed it on the surface of a pure phosphorene, also the sensitivity of the CO gas molecule on the surface of $Al-P$ structure is 3 times small as compared to the adsorbed it on the surface of a pure phosphorene. The $NO/Al-P$ can be excepted as a nanosensor, which represented superior sensitivity and selectivity at a measured 40% as compared to the sensitivity of NO/P at measured 4%. So, phosphorene exhibits high sensitivity to various gases at room temperature. Its sensitivity is influenced by several factors like the material's thickness and whether it's pristine or doped with other elements [35].

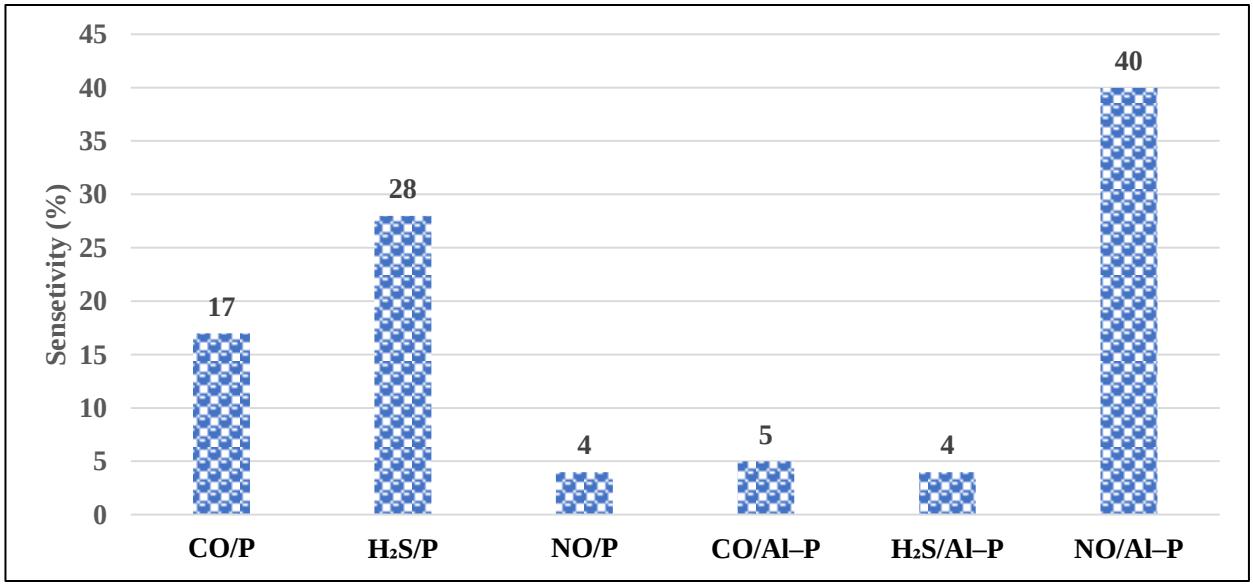

Figure 5. The sensitivity of the adsorbed toxic gases under study (CO, H_2S, and NO) on a pure and aluminium-doped phosphorene at the B3LYP hybrid functional and the 6-31G basis set.

HOMO-LUMO ENERGY LEVELS

To further analyze the effect of gas molecules on the electronic properties of nanocages, the HOMO (highest occupied molecular orbital), LUMO (lowest unoccupied molecular orbital) distributions of Al-P and complexed nanostructures were analyzed. The HOMO primarily serves as an electron donor, while the LUMO primarily serves as an electron acceptor. The red area is negative, the green area is positive.

AL ZAHRAA UNIVERSITY JOURNAL
Health and Medical Science

Al-Zahraa Journal for Health and Medical Sciences 2025; 3:1-21 **Vol. 3, No.3, 2025**
www.zjhms.alzahraa.edu.iq

Figure 6 illustrates the distributions of the frontier molecular orbitals for pure and aluminum-doped phosphorene optimized nanostructures. The energy gap of a pure phosphorene noted is greater than that of Al-doped phosphorene and changed from 1.73 eV to 1.66 eV.

For the LUMO of the Al-phosphorene (Al–P) nanostructure, the positive and negative areas alternated between the inside and outside of the Al and P atoms. The obtained frontier molecular orbital energies (E_{HOMO} and E_{LUMO}) and the calculated energy gap E_g of the (Al–P) nanostructure measured at 1.66 eV, demonstrating its semiconductor properties. After the adsorption of a CO gas molecule on (Al–P), the HOMO of the (CO/Al–P) nanostructure between positive and negative areas more than the LUMO of the (Al–P), this may be due to the high electron transfer in the HOMO level, where the calculated energy gap E_g of the (CO/Al–P) measured at 1.57 eV. In the (H_2S/Al–P) nanostructure, the HOMO and LUMO distributions were localized in the H_2S molecule (especially the H atom with a positive area). This may be because (H_2S/Al–P) has the shortest adsorption distance and the largest transfer charge. The E_g of (H_2S/Al–P) was measured at 1.733 eV. But in the (NO/Al–P) nanostructure, the LUMO distribution was in the NO gas molecule, also may be because (NO/Al–P) has the shortest adsorption distance and the largest transfer charge in the LUMO level such as in Figure 6, where the calculated energy gap E_g of the (NO /P) nanocages measured at 1 eV.

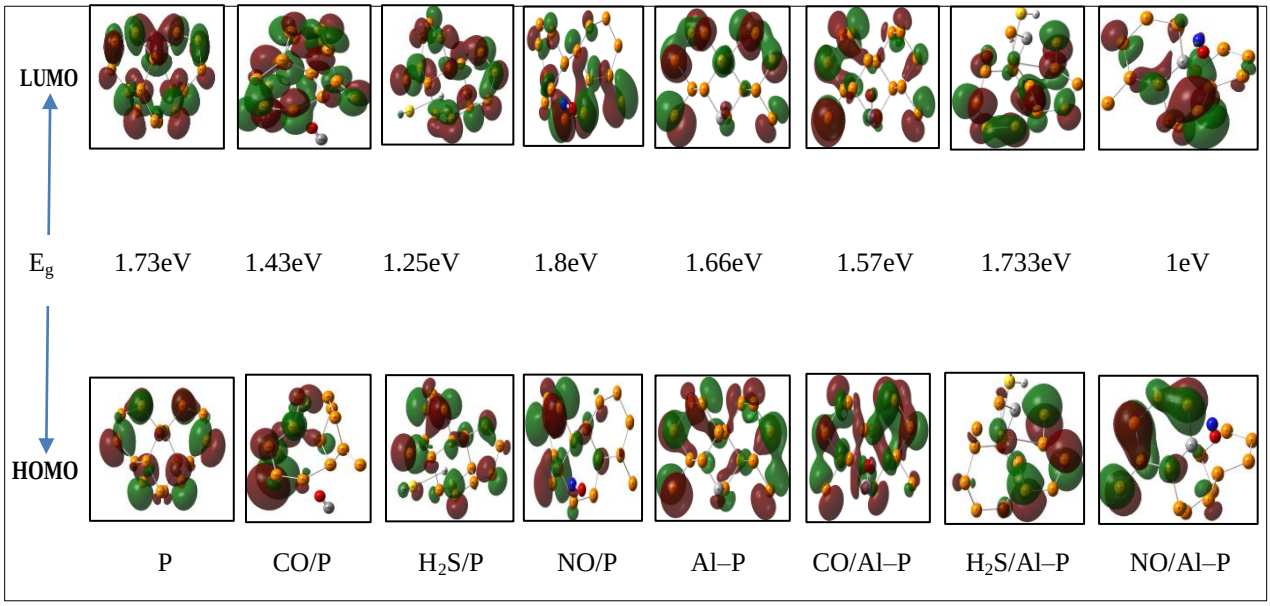

Figure 6. The HOMO- LUMO state of a pure and Al-doped phosphorene nanosheet with and without the toxic gas molecules (CO, H_2S, and NO) at the B3LYP hybrid functional and the 6-31G basis set.

IRAQI Academic Scientific Journals

AL ZAHRAA UNIVERSITY JOURNAL
Health and Medical Science

Al-Zahraa Journal for Health and Medical Sciences 2025; 3:1-21 **Vol. 3, No.3, 2025**
www.zjhms.alzahraa.edu.iq

DENSITY OF STATE (DOS) ANALYSIS

The DOS analysis of the adsorbed gas molecules (CO, H_2S, and NO) on the surface of the pure and aluminum-doped phosphorene nanostructures, simulated using the GaussSum 3.0 software. The DOS spectrum's substantial idea is to explain the shift in the Molecular Orbitals [36]. The diagram of density of state analysis shows the energy (eV) on the x-axis and DOS in arbitrary units (a.u.) on the y-axis. Based on Figure 7, the HOMO–LUMO energy level of aluminium-doped phosphorene Al–P was composed mainly of the 3p orbitals of both P and Al atoms (3s 3p) atom with the energy gap 1.66 eV. After the CO gas molecule adsorbed on the Al-phosphorene (CO/Al–P) has been analyzed, the HOMO–LUMO energy level of CO/Al–P was composed mainly of the 3p orbitals of both P and Al atoms (3s 3p) and 2p orbitals of O and C atoms (2s 2p) with energy gap 1.57 eV. While the H_2S gas molecule adsorbed on a Al-phosphorene (H_2S /Al–P) has been analyzed, as in Figure 3.46, the HOMO–LUMO energy level of H_2S/Al–P was composed mainly of the 3p orbitals of P, Al, and S atoms (3s 3p), and 1s orbitals of H atom (1s) with the energy gap 1.733 eV. So, the effect of the H_2S gas molecular orbital on the H_2S/Al–P nanostructure was not significant. Whereas, after the NO gas molecule adsorbed on the Al-phosphorene (NO/Al–P) has been analyzed, the HOMO–LUMO energy level of NO/Al–P was composed mainly of the 3p orbitals of both P and Al atoms (3s 3p), and the 2p orbitals of N and O atoms (2s 2p) with energy gap 1 eV.

The consideration of only HOMO and LUMO may not yield a realistic description of the frontier orbitals because, in the boundary region, neighboring orbitals may show quasi-degenerate energy levels. For this reason, the total (TDOS), sum of the electron density of states, in terms of Mulliken population analysis, A positive value of the αβDOS indicates a bonding interaction, negative values mean that there is an anti-bonding interaction, and zero values indicate non-bonding interactions, such as in Figure 7.

IRAQI Academic Scientific Journals

AL ZAHRAA UNIVERSITY JOURNAL
Health and Medical Science

Al-Zahraa Journal for Health and Medical Sciences 2025; 3:1-21 **Vol. 3, No.3, 2025**
www.zjhms.alzahraa.edu.iq

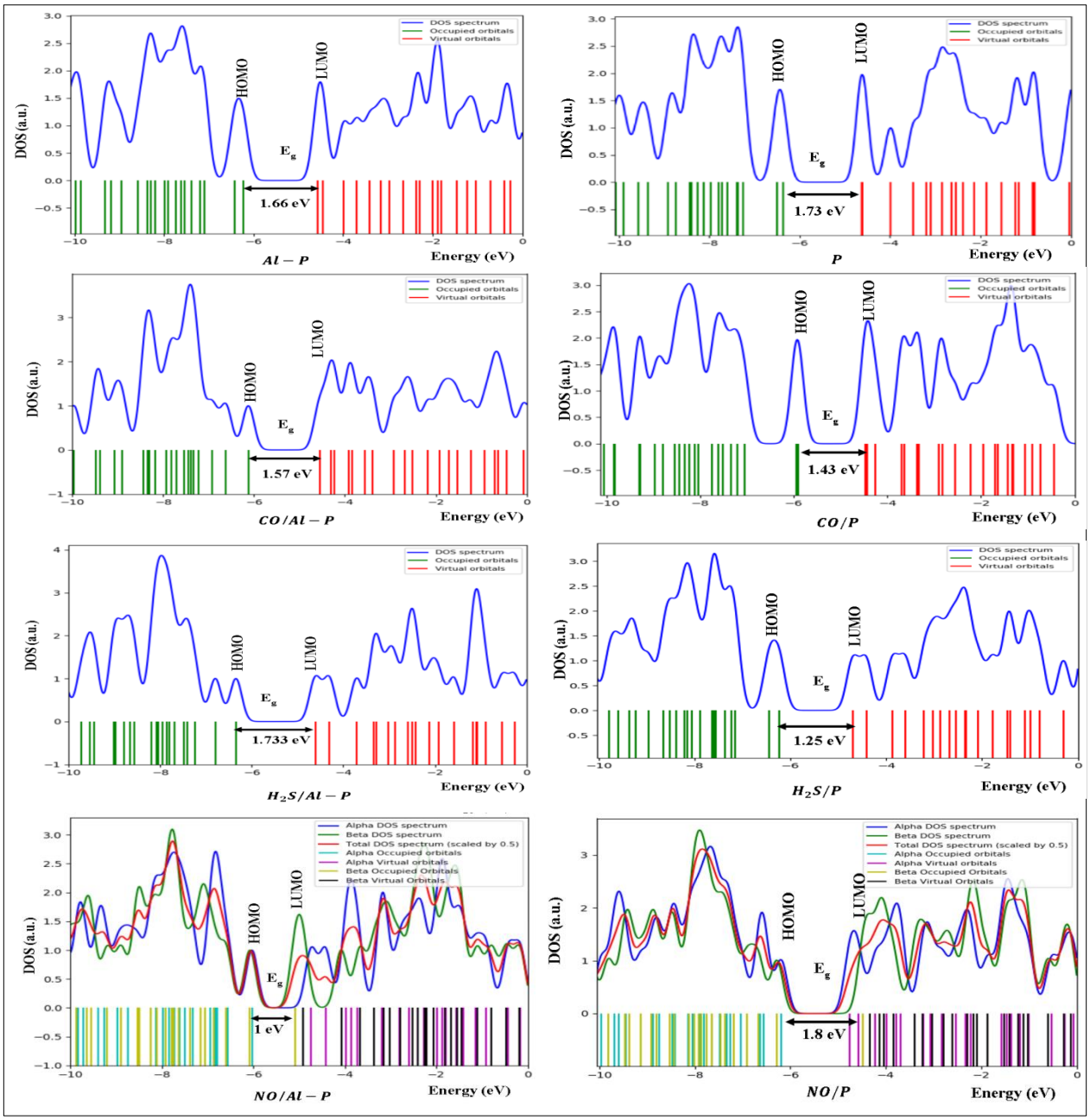

Figure 7. Density of state diagram of a pure and Al-doped phosphorene nanostructure with and without toxic gases.

TD-DFT calculations were performed on the excited-state optimized structures using the 6-31G basis set and the B3LYP hybrid functional. The purpose of investigating the energy gap is to determine the energy of the transition of a pure and aluminum-doped phosphorene with and

IRAQI Academic Scientific Journals

AL ZAHRAA UNIVERSITY JOURNAL
Health and Medical Science

Al-Zahraa Journal for Health and Medical Sciences 2025; 3:1-21 **Vol. 3, No.3, 2025**
www.zjhms.alzahraa.edu.iq

without toxic gases [37]. The energy gap before and after adsorbed toxic gases on a pure and Al-doped phosphorene was found to be in the range 1 –1.733 eV. For a pure phosphorene, the absorption for CO gas molecule is zero with the maximum wavelength is longest at 9400nm that shifted to mid-Infrared spectrum, while the absorption for NO gas molecule is 43a.u. with the maximum wavelength is shortest at 3200nm that shifted to near-Infrared spectrum. While for Al-doped phosphorene, the absorption for NO gas molecule is 5 a.u. with the maximum wavelength measured at 4800nm that shifted to mid-Infrared spectrum, whereas the absorption for H_2S gas molecule is 12a.u. with the maximum wavelength is larges at 7800nm that shifted to near-Infrared spectrum. So, a shift from UV-Vis to Near- and Mid-IR spectrum for phosphorene refers to a change in the type of light absorption. UV-Vis spectroscopy is sensitive to electronic transitions, while IR spectroscopy is sensitive to vibrational transitions. Such as in both Table 1.

Table 1. The UV-Vis. Analysis before and after adsorbed toxic gases under a study (CO, H_2S, NO) on a pure and the Al-doped phosphorene nanostructure at hybrid functional B3LYP and basis set 6-31G.

Nanostructures	Maximum wavelength λ_{max} (nm)	Absorption factor ε (a.u.)	Band gap (eV)
P	5,600	4	1.73
CO/P	9,400	0	1.43
H_2S/P	7,200	8	1.25
NO/P	3,200	43	1.8
Al–P	***6,400***	20	1.66
CO/ Al–P	***5,600***	19	1.57
H_2S/ Al–P	***7,800***	12	1.733
NO/ Al–P	***4,800***	5	1

Figure 8 illustrates the peak of absorption before and after adsorbing toxic gases on the surface of a pure and Al-phosphorene. The spectrum diagram shows the relationship between the maximum wavelength λ_{max} (nm) on the x-axis and the absorption of molecule gases in arbitrary units (a.u.) on the y-axis.

IRAQI Academic Scientific Journals

AL ZAHRAA UNIVERSITY JOURNAL
Health and Medical Science

Al-Zahraa Journal for Health and Medical Sciences 2025; 3:1-21 **Vol. 3, No.3, 2025**
www.zjhms.alzahraa.edu.iq

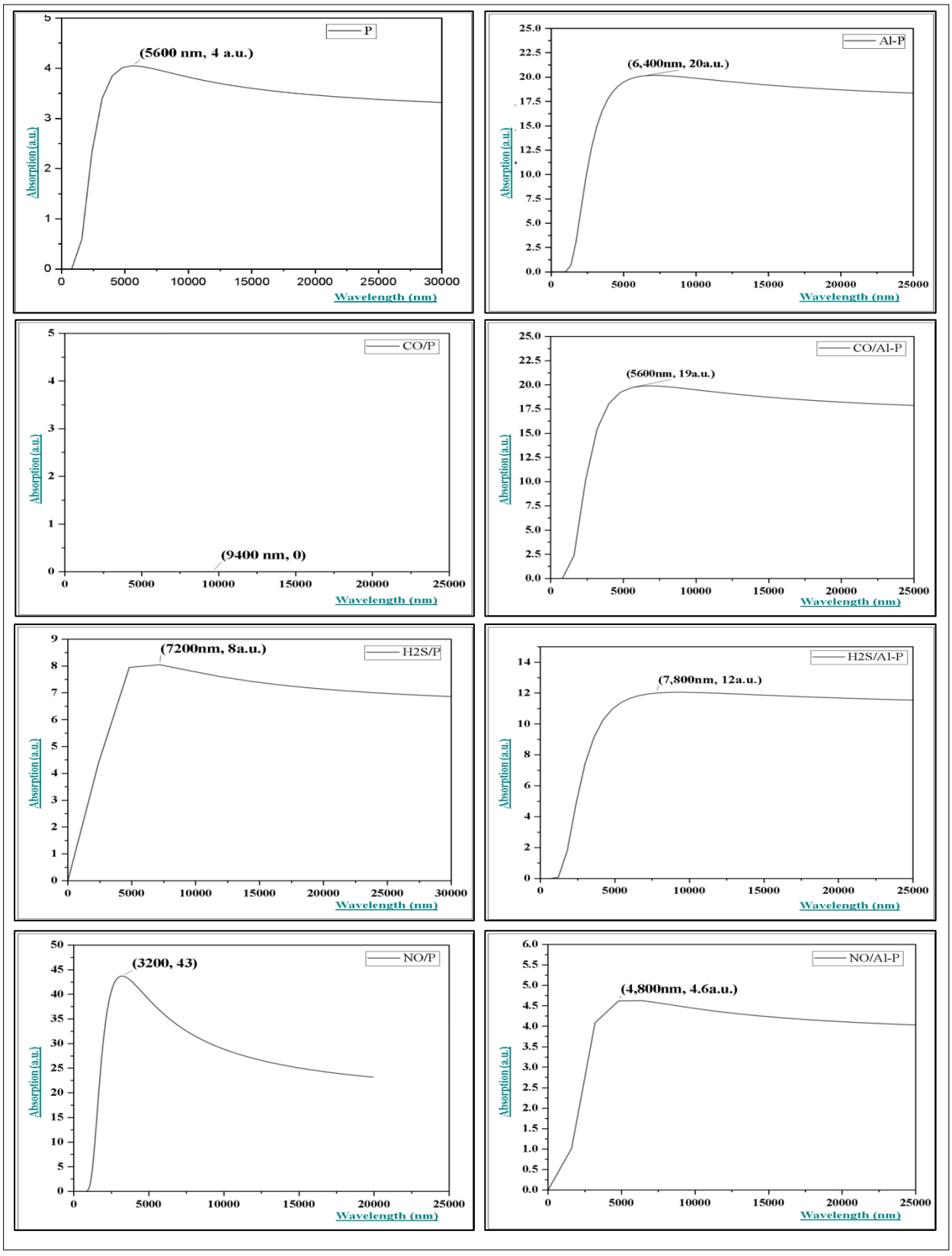

Figure 8. The peak of absorption of UV-Vis. spectrum for all structures of a pure and Al-doped phosphorene.

IRAQI Academic Scientific Journals

AL ZAHRAA UNIVERSITY JOURNAL
Health and Medical Science

Al-Zahraa Journal for Health and Medical Sciences 2025; **3**:1-21 **Vol. 3, No.3, 2025**
www.zjhms.alzahraa.edu.iq

CONCLUSION

In this work, the researcher investigated the nanosensing properties of a pure and Al-doped monolayer phosphorene to know its ability to detect the gas molecules under study using the DFT method at the hybrid function B3LYP and 6-31G basis set. The researcher noted that the energy gap decreased from 1.73 eV for pure phosphorene to 1.66 eV after substituting an aluminum atom with phosphorus atom. Therefore, the sensitivity of nanomaterials depends mainly on the energy gap for the phosphorene nanostructure before and after the adsorption of gas molecules under study. The adsorbed CO, H_2S, and NO gas molecules on the surface of a pure and Al-doped phosphorene nanostructure contributed with varying interactions, especially in the case of H_2S $/Al-P$. Thus, the researcher concluded that Al-phosphorene nanostructures showed the strongest adsorption for H_2S gas molecules reached –2.11 eV. Although the response of an $Al-P$ remains weak for H_2S gas molecules. But the NO/Al-P nanostructures showed the weakest physisorption at +1 eV. So, Al-phosphorene nanostructure can be used as a promising gas detector for nitrogen monoxide NO gas molecule reaching 40%. This indicates that the gas-sensitive needs enough time to obtain the required response according to an exponential curve that depends on the adsorption energy. So, the Al-phosphorene $Al-P$ could be considered a good sensitive nanosensor of NO molecules. And so that the absorption spectra of $NO/Al-P$ cause a shift in the IR spectrum measured at 4,800 nm. Finally, the density of states DOS spectrum for Al-phosphorene nanostructures showed a significant contribution to the unoccupied molecular orbital level. Based on the analysis of the molecular orbitals, $Al-P$ nanostructure can accept more electrons from neighboring atoms. Thus, the NO gas molecule gave the strongest absorption when it was adsorbed with the Al-phosphorene nanostructure.

Acknowledgments: The authors would like to thank all supported people at the University of Kerbala and Al-Zahraa Center for Medical and Pharmaceutical Research Sciences (ZCMRS), Al-Zahraa University for Women.

Conflict of Interest: The authors declare no conflict of interest.

AL ZAHRAA UNIVERSITY JOURNAL
Health and Medical Science

Al-Zahraa Journal for Health and Medical Sciences 2025; **3**:1-21 **Vol. 3, No.3, 2025**
www.zjhms.alzahraa.edu.iq

References

[1] Peruzzini, M., Bini, R., Bolognesi, M., Caporali, M., Ceppatelli, M., Cicogna, F., Coiai, S., Heun, S., Ienco, A., Benito, I.I., Kumar, A., Manca, G., Passaglia, E., Scelta, D., Serrano-Ruiz, M., Telesio, F., Toffanin, S. and Vanni, M. (2018). A Perspective on Recent Advances in Phosphorene Functionalization and Its Applications in Devices. *European Journal of Inorganic Chemistry*, 2019(11-12), pp.1476–1494. doi:https://doi.org/10.1002/ejic.201801219.

[2] Goswami, A. and Gawande, M.B. (2019). Phosphorene: Current status, challenges and opportunities. *Frontiers of Chemical Science and Engineering*, 13(2), pp.296–309. doi:https://doi.org/10.1007/s11705-018-1783-y.

[3] Arbaoui, Z., Boutahir, O., Rahmani, A., Boutahir, M., & Laboratory, A. (2024). Phosphorene: A Promising Two-Dimensional Material for Advanced Electronic Applications. https://primerascientific.com/psen

[4] Islam, M.S., Islam, M.T. and Hossain, M.R. (2024). Phosphorene: A novel nanomaterial revolutionizing biomedicine. *JCIS Open*, [online] 16, p.100124. doi:https://doi.org/10.1016/j.jciso.2024.100124.

[5] Island, J.O., Steele, G.A., Zant, H.S.J. van der and Castellanos-Gomez, A. (2015). Environmental instability of few-layer black phosphorus. *2D Materials*, 2(1), p.011002. doi:https://doi.org/10.1088/2053-1583/2/1/011002.

[6] Kim, J. S., Liu, Y., Zhu, W., Kim, S., Wu, D., Tao, L., Dodabalapur, A., Lai, K. and Akinwande, D. (2015). Toward air-stable multilayer phosphorene thin-films and transistors. *Scientific Reports*, 5(1). doi:https://doi.org/10.1038/srep08989.

[7] Morita, A. (1986). Semiconducting black phosphorus. *Applied Physics A Solids and Surfaces*, 39(4), pp.227–242. doi:https://doi.org/10.1007/bf00617267.

AL ZAHRAA UNIVERSITY JOURNAL
Health and Medical Science

Al-Zahraa Journal for Health and Medical Sciences 2025; **3**:1-21 **Vol. 3, No.3, 2025**
www.zjhms.alzahraa.edu.iq

[8] Liu, H., Du, Y., Deng, Y. and Ye, P.D. (2015). Semiconducting black phosphorus: synthesis, transport properties and electronic applications. *Chemical Society Reviews*, 44(9), pp.2732–2743. doi:https://doi.org/10.1039/c4cs00257a.

[9] Tran, V., Soklaski, R., Liang, Y. and Yang, L. (2014). Layer-controlled band gap and anisotropic excitons in few-layer black phosphorus. *Physical Review B*, 89(23). doi:https://doi.org/10.1103/physrevb.89.235319.

[10] Engel, M., Steiner, M. and Avouris, P. (2014). Black Phosphorus Photodetector for Multispectral, High-Resolution Imaging. *Nano Letters*, 14(11), pp.6414–6417. doi:https://doi.org/10.1021/nl502928y.

[11] Hanley, M.E. and Patel, P.H. (2021). *Carbon Monoxide Toxicity*. [online] PubMed. Available at: https://pubmed.ncbi.nlm.nih.gov/28613491/.

[12] Sawaya, A. and Menezes, R.G. (2021). *Hydrogen Sulfide Toxicity*. [online] Nih.gov. Available at: https://www.ncbi.nlm.nih.gov/books/NBK559264/.

[13] European Commission (2014). *Recommendation from the Scientific Committee on Occupational Exposure Limits for Nitrogen Monoxide*.

[14] Hosseini, S.A. (2025). Phosphorene: an exceptional gas sensor with selective adsorption and distinctive I–V response for NH_3, CH_4, and H_2S. *The European Physical Journal B*, [online] 98(4). doi:https://doi.org/10.1140/epjb/s10051-025-00899-1.

[15] He, H., Hao, Z.-W., Lu, X.-Q., Dong, M.-M., Li, Z.-L., Wang, C.-K. and Fu, X.-X. (2024). Black phosphorene with Au modification: Oxynitride remover and hydrogen sensor. *Applied Surface Science*, 651, pp.159194–159194. doi:https://doi.org/10.1016/j.apsusc.2023.159194.

[16] Ou, P., Song, P., Liu, X. and Song, J. (2018). Superior Sensing Properties of Black Phosphorus as Gas Sensors: A Case Study on the Volatile Organic Compounds. *Advanced Theory and Simulations*, 2(1). doi:https://doi.org/10.1002/adts.201800103.

[17] Tomberg, a. (2009). *Gaussian 09w tutorial an introduction to computational chemistry using G09W and Avogadro software*.

AL ZAHRAA UNIVERSITY JOURNAL
Health and Medical Science

Al-Zahraa Journal for Health and Medical Sciences 2025; **3**:**1**-**21** **Vol. 3, No.3, 2025**
www.zjhms.alzahraa.edu.iq

[18] Mårtensson, J. (2014). *Chemical and Biological Engineering Model Chemistries Getting started Loading GaussView*.

[19] Kim, K. and Jordan, K.D. (1994). Comparison of Density Functional and MP2 Calculations on the Water Monomer and Dimer. *The Journal of Physical Chemistry*, 98(40), pp.10089–10094. doi:https://doi.org/10.1021/j100091a024.

[20] Stephens, P.J., Devlin, F.J., Chabalowski, C.F. and Frisch, M.J. (1994). Ab Initio Calculation of Vibrational Absorption and Circular Dichroism Spectra Using Density Functional Force Fields. *The Journal of Physical Chemistry*, 98(45), pp.11623–11627. doi:https://doi.org/10.1021/j100096a001.

[21] Rassolov, V.A., Ratner, M.A., Pople, J.A., Redfern, P.C. and Curtiss, L.A. (2001). 6-31G* basis set for third-row atoms. *Journal of Computational Chemistry*, 22(9), pp.976–984. doi:https://doi.org/10.1002/jcc.1058.

[22] Tribedi, S., Dang, D.-K., Kanungo, B., Gavini, V. and Zimmerman, P.M. (2023). Exchange correlation potentials from full configuration interaction in a Slater orbital basis. *The Journal of Chemical Physics*, [online] 159(5). doi:https://doi.org/10.1063/5.0157942.

[23] Chen J, Xu Z, Chen Y. (2020). *Electronic structure and surfaces of sulfide minerals : density functional theory and applications*. Amsterdam, Netherlands Elsevier.

[24] Nakamachi, E., Hwang, H., Uetsuji, Y. and Kuramae, H., (2010). Three-scale process-crystallographic analysis of a new biocompatible piezoelectric material $MgSiO_3$ generation. 2 nd International Conference on Computer Technology and Development (pp. 206-210). IEEE. [online] doi:https://doi.org/10.1109/icctd.2010.5645887.

[25] Yu, Z., Lei, S., Wan, N., Luan, S., Shen, H. and Yu, H. (2017). Effect of metal adatoms on hydrogen adsorption properties of phosphorene. *Materials Research Express*, 4(4), pp.045503–045503. doi:https://doi.org/10.1088/2053-1591/aa6ac0.

[26] Alsaati, S.A.A., Abdoon, R.S., Hussein, E.H., Abduljalil, H.M., Mohammad, R.K., Al-Seady, M.A., Jasim, A.N., Saleh, N.A.-H. and Allan, L. (2024). Unveiling the potential of graphene and S-doped graphene nanostructures for toxic gas sensing and solar sensitizer cell

Al-Zahraa Journal for Health and Medical Sciences 2025; **3**:1-21 **Vol. 3, No.3, 2025**
www.zjhms.alzahraa.edu.iq

devices: insights from DFT calculations. *Journal of Molecular Modeling*, 30(6). doi:https://doi.org/10.1007/s00894-024-05994-1.

[27] Sun, M., Hao, Y., Ren, Q., Zhao, Y., Du, Y. and Tang, W. (2016). Tuning electronic and magnetic properties of blue phosphorene by doping Al, Si, As and Sb atom: A DFT calculation. *Solid State Communications*, [online] 242, pp.36–40. doi:https://doi.org/10.1016/j.ssc.2016.04.019.

[28] Yu, Z., Lei, S., Wan, N., Luan, S., Shen, H. and Yu, H. (2017). Effect of metal adatoms on hydrogen adsorption properties of phosphorene. *Materials Research Express*, 4(4), pp.045503–045503. doi:https://doi.org/10.1088/2053-1591/aa6ac0.

[29] Peyghan, A.A., Noei, M. and Tabar, M.B. (2013). A large gap opening of graphene induced by the adsorption of CO on the Al-doped site. *Journal of molecular modeling*, [online] 19(8), pp.3007–14. doi:https://doi.org/10.1007/s00894-013-1832-x.

[30] Zhu, H., Zhou, C., Wang, X., Chen, X., Yang, W., Wu, Y. and Lin, W. (2016). Doping behaviors of adatoms adsorbed on phosphorene. *physica status solidi (b)*, 253(6), pp.1156–1166. doi:https://doi.org/10.1002/pssb.201552586.

[31] Kahn, A. (2016). Fermi level, work function and vacuum level. *Materials Horizons*, 3(1), pp.7–10. doi:https://doi.org/10.1039/c5mh00160a.

[32] Buscema, M., Groenendijk, D.J., Blanter, S.I., Steele, G.A., van der Zant, H.S.J. and Castellanos-Gomez, A. (2014). Fast and Broadband Photoresponse of Few-Layer Black Phosphorus Field-Effect Transistors. *Nano Letters*, 14(6), pp.3347–3352. doi:https://doi.org/10.1021/nl5008085.

[33] Upadhyay, S. and Srivastava, P. (2022). Enhanced DFT insights of doped phosphorene: Structural and electronic considerations. *Computational and Theoretical Chemistry*, 1214, p.113754. doi:https://doi.org/10.1016/j.comptc.2022.113754.

[34] Torres, I., Mehdi Aghaei, S., Rabiei Baboukani, A., Wang, C. and Bhansali, S. (2018). Individual Gas Molecules Detection Using Zinc Oxide–Graphene Hybrid Nanosensor: A DFT Study. *C*, 4(3), p.44. doi:https://doi.org/10.3390/c4030044.

AL ZAHRAA UNIVERSITY JOURNAL
Health and Medical Science

Al-Zahraa Journal for Health and Medical Sciences 2025; **3**:**1**-**21** **Vol. 3, No.3, 2025**
www.zjhms.alzahraa.edu.iq

[35] Aasi, A., Aghaei, S.M. and Panchapakesan, B., (2021). Pt-decorated phosphorene as a propitious room temperature VOC gas sensor for sensitive and selective detection of alcohols. *Journal of Materials Chemistry C*, 9(29), pp.9242–9250. doi:https://doi.org/10.1039/d1tc01510a.

[36] Kadhim, Q., Abdoon, R., Mohammed, H., Abbas, A., Al-Seady, M., Nagy, G., Abduljalil, H., Saleh, N.A. H. and Kahaly, M. (2022). Effect of metal ad-atoms on the structural, electrical, and optical properties of boron-nitride nanostructures towards optoelectronics: a DFT based study. *Egyptian Journal of Chemistry*, [online] 0(0). doi:https://doi.org/10.21608/ejchem.2022.130936.5763.

[37] Ajeel, F.N., Mohammed, M.H. and Khudhair, A.M. (2019). Effects of Lithium impurities on electronic and optical properties of graphene nanoflakes: a DFT–TDDFT study. *Chinese Journal of Physics*, [online] 58. doi:https://doi.org/10.1016/j.cjph.2019.01.009.